Title
Mfge8 is critical for mammary gland remodeling during involution

Journal
Molecular Biology of the Cell, 16(12)

ISSN
1059-1524

Authors
Atabai, Kamran
Fernandez, Rafael
Huang, Xiaozhu
et al.

Publication Date
2005-12-01

Peer reviewed

Molecular Biology of the Cell
Vol. 16, 5528–5537, December 2005

Mfge8 Is Critical for Mammary Gland Remodeling during Involution

Kamran Atabai,*† Rafael Fernandez,*† Xiaozhu Huang,*† Iris Ueki,† Ahnika Kline,*† Yong Li,*† Sepid Sadatmansoori,*† Christine Smith-Steinhart,‡§ Weimin Zhu,‖ Robert Pytela,‖ Zena Werb,¶ and Dean Sheppard*†

*Lung Biology Center, Cardiovascular Research Institute and Departments of †Medicine and ¶Anatomy, University of California–San Francisco, San Francisco, CA 94143; ‡Department of Immunology, §National Jewish Medical Center and §Department of Medicine, University of Colorado Health Science Center, Denver, CO 80206; and ‖Epitomics, Burlingame, CA 94010

Submitted February 15, 2005; Revised August 17, 2005; Accepted September 15, 2005
Monitoring Editor: M. Bishr Omary

Apoptosis is a critical process in normal mammary gland development and the rapid clearance of apoptotic cells prevents tissue injury associated with the release of intracellular antigens from dying cells. Milk fat globule-EGF-factor 8 (Mfge8) is a milk glycoprotein that is abundantly expressed in the mammary gland epithelium and has been shown to facilitate the clearance of apoptotic lymphocytes by splenic macrophages. We report that mice with disruption of *Mfge8* had normal mammary gland development until involution. However, abnormal mammary gland remodeling was observed postlactation in *Mfge8* mutant mice. During early involution, *Mfge8* mutant mice had increased numbers of apoptotic cells within the mammary gland associated with a delay in alveolar collapse and fat cell repopulation. As involution progressed, *Mfge8* mutants developed inflammation as assessed by CD45 and CD11b staining of mammary gland tissue sections. With additional pregnancies, *Mfge8* mutant mice developed progressive dilatation of the mammary gland ductal network. These data demonstrate that Mfge8 regulates the clearance of apoptotic epithelial cells during mammary gland involution and that the absence of Mfge8 leads to inflammation and abnormal mammary gland remodeling.

INTRODUCTION

Milk fat is synthesized by differentiated mammary gland epithelial cells and secreted into the ductal lumen enveloped in a portion of the apical plasma membrane termed the milk fat globule membrane (MFGM; Mather, 1987). The MFGM is made up of glycoproteins, proteins, cholesterol, and phospholipids. In addition to providing nutrition, milk proteins have antimicrobial and antiviral activity, promote the growth of beneficial bacteria, and aid in the development of the neonatal digestive tract (Mather, 1987; Lonnerdal, 2003). Milk proteins may also play a role in mammary gland development. Whey acidic protein and β-casein, two of the most abundant milk proteins, serve as classical markers of epithelial cell differentiation and a developmental role has been suggested for whey acidic protein (Shamay *et al.*, 1992; Hirai *et al.*, 1998; Ikeda *et al.*, 2002).

Milk fat globule-EGF- factor 8 (Mfge8) is a glycoprotein that makes up part of the MFGM (Stubbs *et al.*, 1990). Mfge8 found in mouse mammary gland milk consists of a long and short (Mfge8L and Mfge8S) isoform (Oshima *et al.*, 1999). Both isoforms have two N-terminal Notch-like EGF domains. The second EGF-like domain is highly conserved across species and contains an arginine-glycine-aspartic acid (RGD) sequence that has been shown to bind the $\alpha v\beta 3$ and $\alpha v\beta 5$ integrins (Hanayama *et al.*, 2002). The EGF-like domains are followed by two discoidinlike Factor 5/Factor 8 domains. The carboxyl-terminal discoidin domains bind phosphatidylserine residues expressed on the surface of apoptotic cells and are essential for Mfge8-mediated uptake of these cells (Hanayama *et al.*, 2002). Mfge8L contains an additional proline-threonine-rich domain inserted between the EGF-like and discoidin domains. Mammary gland Mfge8L transcripts increase with pregnancy and lactation suggesting a specific role for this isoform in the pregnant and lactating mammary gland (Oshima *et al.*, 1999).

Initial interest in Mfge8 focused on lactadherin, the human orthologue of Mfge8, and its potential role in mammary gland carcinomas (Larocca *et al.*, 1991; Carmon *et al.*, 2002). More recently, Mfge8 has been shown to facilitate in vitro phagocytosis of apoptotic T-cells by activated peritoneal macrophages and to enhance the in vivo clearance of apoptotic lymphocytes by splenic macrophages (Hanayama *et al.*, 2002, 2004).

The importance of apoptosis throughout mammary gland development (Strange *et al.*, 2001) and the ability of Mfge8 to facilitate the clearance of apoptotic leukocytes suggests a potentially important function for Mfge8 in mammary gland development. Though apoptosis is critical in prepregnancy mammary gland development (Humphreys *et al.*, 1996, 1999), the tissue remodeling that takes place during mammary gland involution requires programmed cell death and removal of ~90% of the mammary gland epithelium (Wiseman and Werb, 2002). Despite this massive cell turnover, mammary gland involution is nearly complete by 10 d, at which time there is scant evidence of apoptotic cells (Fadok,

This article was published online ahead of print in *MBC in Press* (http://www.molbiolcell.org/cgi/doi/10.1091/mbc.E05–02–0128) on September 29, 2005.

Address correspondence to: Dean Sheppard (dean.sheppard@ucsf.edu).

1999). For involution to proceed in an orderly manner apoptotic cells must be cleared quickly and completely and milk remaining in the ductal lumen must be reabsorbed (Wilde *et al.*, 1999). As epithelial cells undergo apoptosis they are phagocytosed by adjacent epithelial cells or are shed into the ductal lumen where they are engulfed by phagocytic cells (Monks *et al.*, 2005). Mfge8 on the milk membrane and on the apical surface of viable epithelial cells is in close proximity with apoptotic epithelial cells and is in the ideal location to facilitate rapid and orderly clearance of these cells.

In this study we have generated mice homozygous for a gene trap mutation that disrupts *Mfge8* and eliminates the carboxy terminal discoidin domain (Silvestre *et al.*, 2005). Here we report that despite normal mammary gland development during puberty, *Mfge8* mutant mice fail to rapidly clear apoptotic cells and develop progressive inflammation during involution coupled with destruction of mammary gland architecture after successive pregnancies. These studies show that Mfge8 plays a central role in orchestrating postlactational mammary gland remodeling.

MATERIALS AND METHODS

Generation of Mfge8 *Mutant Mice*

Mfge8 mutant mice were generated by blastocyst injection of KST227 embryonic stem cells that harbor an insertion of the pGT1-pfs gene trap-vector in intron 7 of *Mfge8* (Silvestre *et al.*, 2005). The pGT1-pfs vector is designed to trap secretory proteins at the cell surface through its transmembrane domain. Southern blot experiments using a digoxin-labeled (Roche, Indianapolis, IN) genomic probe (forward 5′ CTGTTCTGATGGTGGTGGTG and reverse 5′ TAAGCACCCACGTGTTTGAG) spanning a 580-base pair segment flanking exon 7 detected a 10.5-kb *Bam*HI fragment for the wild-type allele and an ~2.5-kb fragment for the mutant allele. Subsequent genotyping was done by PCR. A forward primer K2 (5′ TTCTTTCCCTTCAATGGCAC) and the reverse primer R4 (5′ CCATATTCCCACGTTTGACC) generated a 402-base pair product for the wild-type allele and the forward primer K2 and the reverse primer R73 (5′ CGTGTCCTACAACACACACTCCAACC) from the gene trap-vector produced an ~260-base pair product for the targeted allele.

Animal Husbandry

Mice were housed at the animal care facility at the University of California San Francisco and all studies were approved by the institutional review board. Mice were maintained on a mixed C57/BL6:129 OLA background. Mutant animals were generated from heterozygous intercrosses and from homozygous-heterozygous mating pairs. For studies of mammary gland development, 8-wk-old and 9-mo-old nulliparous females and age matched littermates at estrus (as determined by vaginal smear) were used. Age-matched littermates at first pregnancy were used for studies of pregnancy, lactation, and involution and litter size was normalized to four pups for studies of lactation and involution. Studies of apoptosis during involution were done on mice at first pregnancy with forced involution after 10 d of lactation. Heterozygote mice served as controls in these studies.

β-Galactosidase Staining

Frozen sections, 5 μm, were air dried and fixed with 10% neutral buffered Formalin and incubated in X-gal solution in a humidity chamber at 37°C overnight. X-gal solution consisted of 1:30 dilution of X-gal stock (30× X-gal reagent, Pierce, Rockford, IL) in 5 mM potassium ferrocyanide crystalline, 5 mM potassium ferrocyanide trihydrate, and 2 mM magnesium chloride in phosphate-buffered saline (PBS). Slides were rinsed with PBS and immersed in 100% ethanol until all precipitate dissolved, counterstained with Eosin Y, and dehydrated and mounted.

Reverse Transcription-PCR

RNA was isolated from mouse mammary gland using Trizol reagent (Invitrogen, Carlsbad, CA) according to the manufacturer's instructions. Single-stranded cDNA was transcribed from 3 μg of RNA using the superscript first-strand synthesis system (Invitrogen) and random hexamers. PCR was performed using primers covering exon 7 and 8 (forward primer 5′CGCAAGTTTGAGTTCATCCA, reverse primer 5′GCATTGATCTTGCCCTGATT).

Development of Monoclonal Antibody to Mfge8

The rabbit monoclonal antibody (mAb) 4F6 was generated by immunizing a rabbit with mouse mammary tumor cells from MMTV-PyVmT-transgenic mice. Splenocytes from immunized rabbits were fused with rabbit plasmacytoma 240E cells and the resultant hybridomas were screened by immunohistochemistry with tissue sections from mouse mammary tumors. The 4F6 antibody stained both normal and malignant mammary epithelium. Specificity for Mfge8 was demonstrated because, as shown by immunocytochemistry, the antibody strongly reacted with HEK-293 cells transfected with an Mfge8 cDNA expression vector, but not with mock-transfected HEK-293 cells (unpublished data). Antibody specificity was confirmed by Western blot analysis of mammary tumor cell lysates, showing a pattern of bands consistent with the previously described molecular forms of Mfge8.

Whole Mount Preparation

The inguinal mammary gland was removed and fixed overnight in Carnoy's solution (3:1 ratio of alcohol/glacial acetic acid), hydrated, and stained overnight with carmine alum (0.2% carmine dye and 0.5% aluminum potassium sulfate), dehydrated, defatted with xylene, mounted and photographed. For evaluation of ductal diameter, whole mounts from mice greater than 10 d postinvolution were photographed and the diameter of the largest primary duct along its course adjacent to the central lymph node (5–15 measurements per duct) was measured using NIH image 1.63.

Morphometry

For morphometric evaluation of epithelial and fat content of the mammary gland, 5-μm sections were stained with hematoxylin and eosin (H & E), and images were obtained from 10 randomly selected fields (Leica, Deerfield, IL; DM 5000 B, 100×) using SPOT software. A grid was superimposed on the digital images and the number of intersections that marked epithelium and adipocytes was counted and expressed as a percentage. The investigator was blinded to the genotype of the sections. For evaluation of the phagocytic index of epithelial cells, 5-μm sections from day 2 of involution were stained with H & E and the number of ingested particles within alveolar epithelial cells was counted from 10 randomly chosen high-powered fields using an oil objective (1000×). Ingestions were counted as apoptotic particles if a whole apoptotic cell or a round apoptotic body with a clear rim surrounding it (spacious phagosome) was observed within the cytoplasm of an epithelial cell lining the alveolar lumen (Monks *et al.*, 2005). The phagocytic index was calculated as the number of ingested particles multiplied by the proportion of epithelial cells with ingested particles. The investigator was blinded to the genotype of the sections.

Immunohistochemistry and Immunofluorescence

Mammary glands were removed and fixed in 4% paraformaldehyde overnight and then embedded in paraffin. For H & E staining, 5-μm sections were rehydrated and stained according to standard protocols. For immunohistochemistry, 5-μm sections were boiled for 15 min in 10 mM sodium citrate (pH 6) for antigen retrieval and blocked with H_2O_2 in methanol and subsequently 2% bovine serum albumin. Rabbit mAb (4F6) directed against Mfge8 was used at 1:20 dilution in PBS and 0.5% Tween, followed by a 1:200 biotinylated anti-rabbit secondary antibody (Vector, Burlingame, CA), ABC reagent (Vector), and liquid diaminobenzidine substrate (Sigma, St. Louis, MO). For CD45 staining, a rat anti-mouse mAb (BD Biosciences, San Diego, CA; 1:100 dilution) was used. TUNEL assay was done using a kit from Chemicon (Apoptag; Temecula, CA) and following manufacturer's instructions. For immunofluorescence, apoptotic cells obtained from mammary gland milk were washed with PBS and cytospin preparations were fixed with 3% PFA and 3% sucrose in PBS, blocked with 5% donkey serum, incubated overnight with anti-activated caspase 3 antibody (1:50 dilution, Cell Signaling, Beverly, MA) at 4°C, and incubated with a FITC-conjugated secondary antibody (1:100 dilution, Jackson Laboratories, West Grove, PA) and 4′,6-diamidino-2-phenylindole (DAPI). For immunofluorescence staining of the mammary gland, 5-μm sections of mammary gland tissue frozen in OCT were air dried, fixed in 1% PFA and 3% sucrose, blocked in 5% goat serum, and incubated with anti-CD11b antibody (Serotec, Raleigh, NC; 1:100 dilution) for 1 h followed by 1-h incubation with a FITC-conjugated goat anti-rat antibody (1:100 dilution, Jackson Laboratories) and DAPI.

Quantification of Apoptotic and Inflammatory Cells

Apoptotic cells in the mammary gland were identified by TUNEL assay and morphological criteria. The percentage of apoptotic nuclei was quantified by combining the number of apoptotic cells in the alveolar lumens on H & E-stained sections and the number of TUNEL-positive cells on tissue sections from 14 randomly selected high-power fields (HPF, 400×). The number of CD45- and CD11b-positive cells per HPF (400×) was counted on 10–14 randomly selected fields. Investigators were blinded to the genotype of the sections examined.

Cell Culture

Primary mammary gland epithelial cells (PMEC) were obtained from 3-mo-old *Mfge8* mutant and heterozygous control mice during the third week of pregnancy. Mammary glands were minced and digested with 0.1% collagenase type 3 (Worthington, Lakewood, NJ) and 0.2% trypsin in DMEM/F12

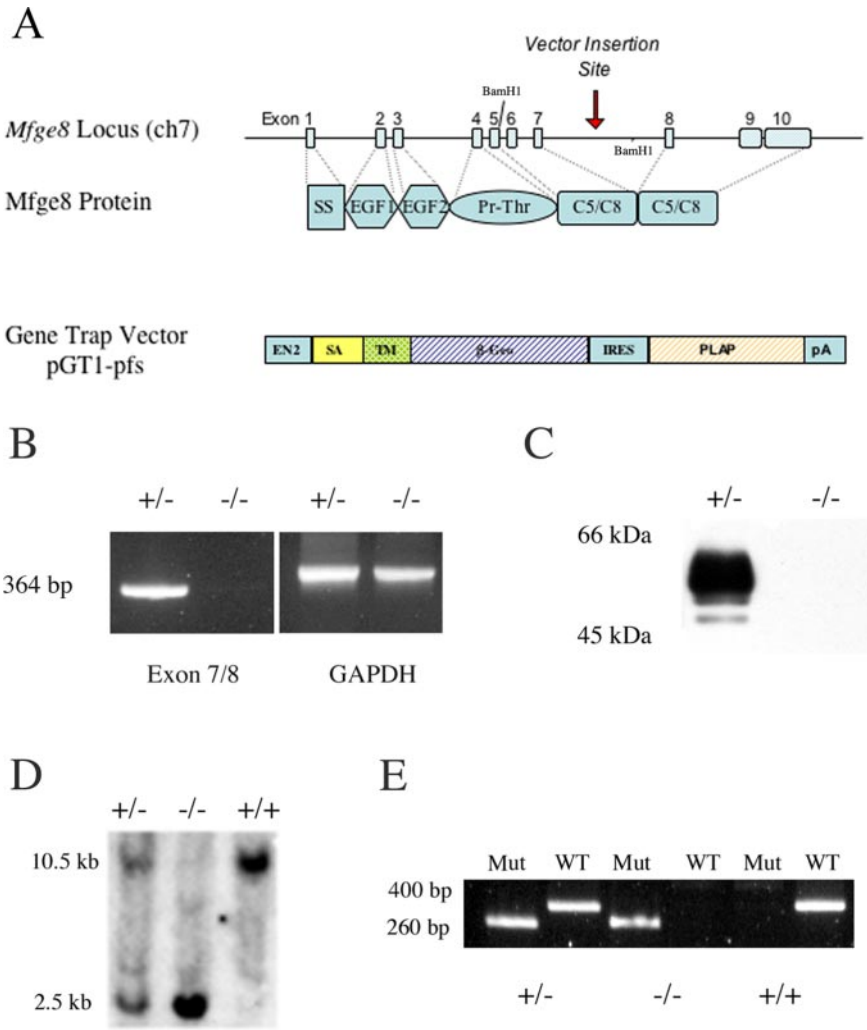

Figure 1. Generation of Mfge8 mutant mice. (A) Wild-type allele of *Mfge8* showing the location of the EGF-like, proline-threonine rich, and C5/C8 domains and the gene trap-vector pGTI-pfs. Note the insertion site of the gene trap-vector between exon 7 and exon 8. The gene trap-vector has an engrailed-2 domain (en-2) followed by a splice acceptor site (SA), a CD4 transmembrane domain (TM), a β-galactosidase-neomycin fusion gene (βgeo), an internal ribosomal entry site (IRES), a placental alkaline phosphatase domain (PLAP), and a polyadenylation domain (pA). (B) RT-PCR with primers spanning the vector insertion site showed the expected 364-base pair (base pairs) product in the heterozygote mouse but not the homozygote mouse. (C) Western blot using 4F6 antibody showed the expected band in the heterozygote but not homozygote mouse. (D) Southern blot using a digoxin-labeled genomic probe after digestion of tail DNA with *Bam*HI show a 10.5-kb (kb) band in wild-type allele and an ~2.5-kb band in the mutated allele. (E) PCR using a single forward primer and two reverse primers identify a 402-base pairs band for the wild-type allele and an ~260-base pairs band for the mutated allele.

supplemented with 5% fetal calf serum (FCS) and 100 U/ml penicillin and 100 μg/ml streptomycin for 1–2 h. The digests were passed through a 500-μm filter (Sefar, Buffalo, NY) and washed with DMEM/F12. Several 30-s centrifugation steps were used to remove single cells. Mammary gland organoids were plated on eight-well chamber slides (LabTek, Naperville, IL) precoated for 1 h with type 1 collagen (Sigma) in complete medium (DMEM/F12 supplemented with 5% FCS, 5 μg/ml insulin, Sigma; 100 ng/ml hydrocortisone, Sigma; 25 ng/ml EGF, R&D, Minneapolis, MN; and 100 U/ml penicillin and 100 μg/ml streptomycin). The organoids formed monolayers 72–96 h after plating.

Phagocytic Assay

Apoptotic epithelial cells were obtained from the milk of *Mfge8* mutant and control mice 24 h after forced involution. Mice were anesthetized with ketamine (100 mg/kg) and xylazine (10 mg/kg) and injected with oxytocin (0.01 USP units/g body weight) 15 min before milking. Milk was obtained by gentle manual pressure and collected into a sterile tube on ice using a pipette. Milk was mixed with a 1:1 dilution of DMEM/F12 and centrifuged at 3000 rpm for 5 min. After removing the supernatant, cells were washed twice with DMEM/F12 and resuspended and counted in complete medium. Milked apoptotic cells (n = 200,000) suspended in 350 μL of complete medium were added to each well of PMEC monolayers, and experiments were carried out in duplicate wells. Milked apoptotic cells from homozygous mice were incubated with PMEC monolayers from homozygous mice and milked apoptotic cells from heterozygous mice were incubated with PMEC monolayers from heterozygous mice. Five hours after incubation, wells were washed vigorously with PBS to remove bound apoptotic cells and stained with Dif-Quick. The phagocytic index was quantified by counting ingestions from 30 high power fields (1000×) selected at random from duplicate wells. Cells were considered ingested if the whole apoptotic cell surrounded by a clear vacuole was visible within epithelial cells in the monolayers. Bound cells and small particles were not counted.

Western Blot Analysis

Freshly isolated mammary gland tissue was snap frozen in liquid nitrogen and subsequently homogenized in RIPA buffer (150 mM NaCl, 20 mM Tris-HCl, pH 7.6, 1% NP-40, 0.5% deoxycholate, and 0.1% SDS, 1 mM phenylmethylsulfonyl fluoride, and complete mini protease inhibitor cocktail tablets, Amersham, Piscataway, NJ). The homogenates were centrifuged for 10 min at 4°C and the supernatant stored at −80°C. Eighty micrograms of protein was separated on 8, 10, or 12% polyacrylamide gels, transferred to an Immobilon membrane, and blocked overnight with 5% milk in TBST (20 mM Tris, pH 7.6, 150 mM NaCl, and 0.1% Tween). 4F6 antibody (1:50 dilution), anti-β-galactosidase antibody (AbCam, Cambridge, UK; 1:2000 dilution), anti-C/EBPβ antibody (Santa Cruz Biotechnology, Santa Cruz, CA; 1:500 dilution), anti-β-actin (Sigma, 1:5000 dilution) or anti-epimorphin antibody (Stressgen, Victoria, British Columbia, Canada; 1:20,000 dilution) was followed by horseradish peroxidase-conjugated anti-rabbit or anti-mouse secondary antibody (Amersham) at 1:5000 dilution. Blots were developed using enhanced chemiluminescence reagents (Amersham).

RESULTS

Generation of Mfge8 *Mutant Mice by Gene Trap Strategy*

The gene trap vector pGT1-pfs inserted in intron 7 of Mfge8 (Figure 1A) to produce a 209 kDa fusion protein containing the first 269 amino acids of Mfge8 followed by β-galactosidase protein. β-galactosidase protein expression was detected in the mammary gland epithelium (Figure 2, B and D) and also in the heart, lung, spleen, brain, kidney, skin, and skeletal muscle (unpublished data). RT -PCR using primers

spanning exons 7 and 8 showed the expected 364 base pair product in heterozygote but not homozygote mutant mice (Figure 1B). Western blots using an antibody (4F6) directed against Mfge8 showed a band at ~66 and 53 kDa representing Mfge8L and Mfge8S in heterozygote mice but no band in homozygous mice, suggesting that the epitope recognized by this antibody is in the carboxyl terminal region of Mfge8 deleted by this insertion (Figure 1C). Genotyping was performed initially by Southern Blot (Figure 1D) and subsequently by PCR (Figure 1E).

Given the role of Mfge8 in sperm-egg binding (Ensslin and Shur, 2003), we counted the number of offspring born to homozygote and heterozygote males paired with heterozygote females. As previously reported for *Mfge8* null mice generated by a different targeting strategy (Ensslin and Shur, 2003), male *Mfge8* mutant mice were hypofertile (unpublished data). In addition, as reported for another *Mfge8*-null mouse line (Hanayama *et al.*, 2004), *Mfge8* mutants developed age-dependent splenomegaly and had impaired macrophage-mediated engulfment of apoptotic thymocytes (Silvestre *et al.*, 2005), suggesting that our line of *Mfge8* mutants is functionally equivalent to the traditional knockouts.

Mfge8 Fusion Protein Is Trapped Intracellularly

To evaluate whether the pGT1-pfs gene trap vector produced a fusion protein of the expected size (209 kDa), we performed Western blots on mammary gland lysates from day 2 of involution using an anti-β-galactosidase antibody. An ~209-kDa band representing the fusion protein was found in heterozygous and homozygous females but not in wild-type females (Figure 2A). A second band at ~170 kDa was present in heterozygous and homozygous females but not in wild-type females and likely represented a degradation product of the fusion protein. To determine whether the fusion protein was successfully trapped intracellularly, we stained for β-galactosidase expression in tissue sections from heterozygote females. The fusion protein, as seen here on day 10 of lactation, was restricted to the cell surface of the alveolar and ductal epithelium (Figure 2, B and D). In contrast, native Mfge8, detected using a mAb, showed the protein in the lumen and apical surface of alveolar and ductal epithelium (Figure 2, C and E).

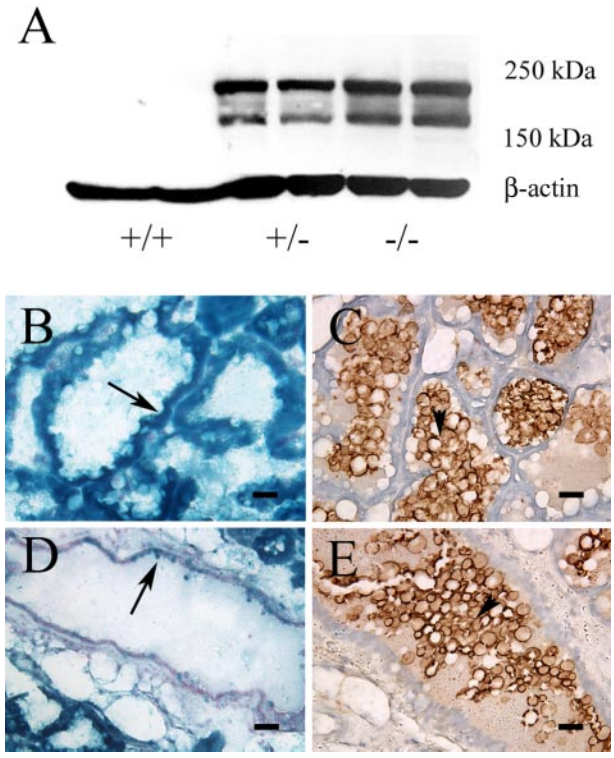

Figure 2. The pGTI-pfs vector produces a fusion protein that is trapped intracellularly. (A) Western blot of mammary gland lysis from day two of involution using a polyclonal rabbit anti-β-galactosidase antibody identified a band at 209 kDa, the predicted weight of the Mfge8 fusion protein, in heterozygous and homozygous mice but not in wild-type (WT) mice. (B–E) The transmembrane domain of the pGTI-pfs vector was designed to trap secretory proteins intracellularly. (B and D) β-galactosidase staining of a heterozygote female on day 10 lactation showed the fusion protein produced by the vector trapped intracellularly in the alveolar and ductal epithelium (arrows in B and D). (C and E) In contrast, the native protein, stained with an anti-Mfge8 antibody, was localized to the lumen and apical surface of the alveolar and ductal epithelium (arrowheads in C and E). Bar, 0.1 mm.

Mfge8 *Mutant Mice Have Normal Development during Puberty, Pregnancy, and Lactation*

We first examined mammary gland morphology during various developmental stages. At 4 wk of age, the morphology of the ductal network was variable but we did not observe any consistent differences between homozygote mutants and heterozygote controls in ductal morphology or depth of penetration of the fat pad relative to the central lymph node (Figure 3, A and B). At 8 wk of age, homozygous mice at estrus occasionally had ductal ectasia and dilatation but the majority of mutants and controls had similar ductal and parenchymal morphology as heterozygous controls as assessed by whole mount and histological sections (unpublished data). Histological and whole mount analysis revealed no obvious differences on pregnancy day 18.5 (Figure 3, C and D, and unpublished data) and lactation day 10 (Figure 3, E and F, and unpublished data). Morphometric quantification of epithelial content revealed no differences between homozygous and heterozygous females at 8 wk of age, pregnancy day 18.5, or lactation day 10 (Figure 3G).

Alveolar Collapse and the Repopulation of Adipocytes during Involution Are Delayed in **Mfge8** *Mutant Mice*

Mammary gland involution requires complete reorganization of the parenchyma at a time during which Mfge8 protein expression is maximal (unpublished data). We examined H & E-stained sections of days 1–5 of involution. On day 1 of involution, *Mfge8* mutants had many more apoptotic bodies in the alveolar lumens (Figure 4, A and B). On day 2 there was a continued excess of apoptotic bodies coupled with a delay in alveolar collapse and fat cell repopulation of the mammary gland parenchyma (Figure 4, C, D, and G). By day 3, *Mfge8* mutants and heterozygote controls had a similar histological appearance that persisted through day 5 (Figure 4, E, F, and G, and unpublished data).

Mfge8 *Mutants Have Increased Numbers of Apoptotic Cells in Involution*

One striking difference was the apparent increase in apoptotic cells in the involuting mammary gland. To quantify the proportion of apoptotic cells, we counted the total number of apoptotic cells during involution (Figure 5, A–C). *Mfge8* mutants had an increase in the percentage of apoptotic

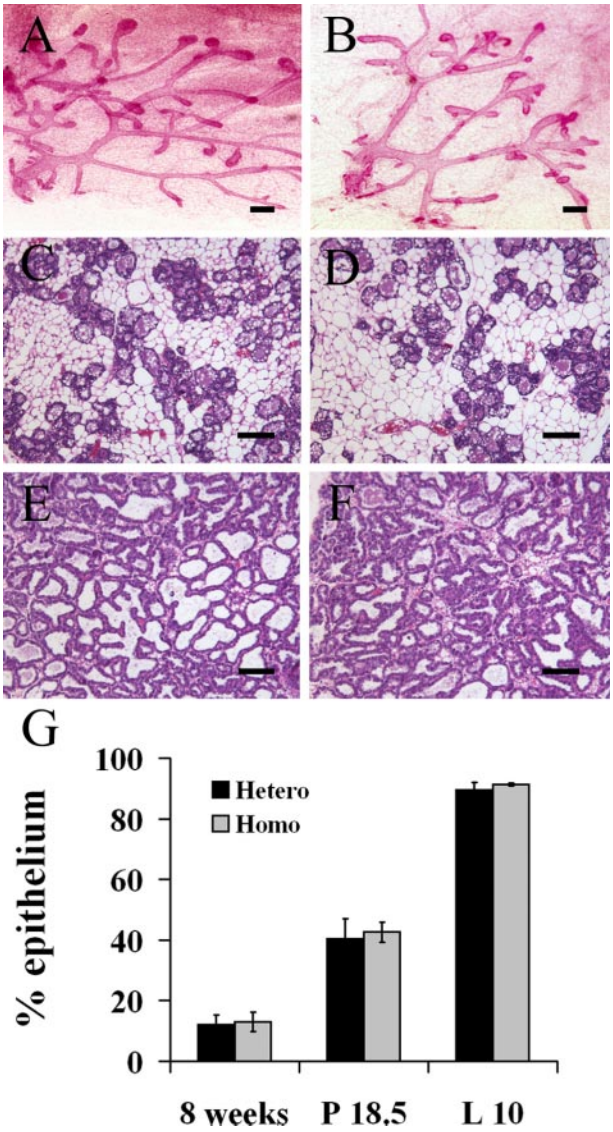

Figure 3. *Mfge8* mutant mice have normal mammary gland development through lactation. (A and B) Whole mounts of mammary gland from 4-wk-old heterozygote (A) and homozygote (B) mice did not show any difference in ductal morphology. (C–F) *Mfge8* mutant mice did not show any phenotype on H & E sections of pregnancy day 18.5 (D) or lactation day 10 (F) compared with heterozygote controls (C and E). Whole mounts from pregnancy day 18.5 and lactation day 10 were similar in homozygote and heterozygote controls (unpublished data). (G) The epithelial content of the mammary gland was quantified by superimposing a grid on 10 randomly selected fields (100×) and counting the number of intersections that marked epithelium or adipose tissue. No differences were found in Mfge8 mutant and control mice at 8 wk of age (at estrus), on pregnancy day 18.5 (P 18.5), or lactation day 10 (L 10, n = 3 for each group). Bar, 0.2 mm.

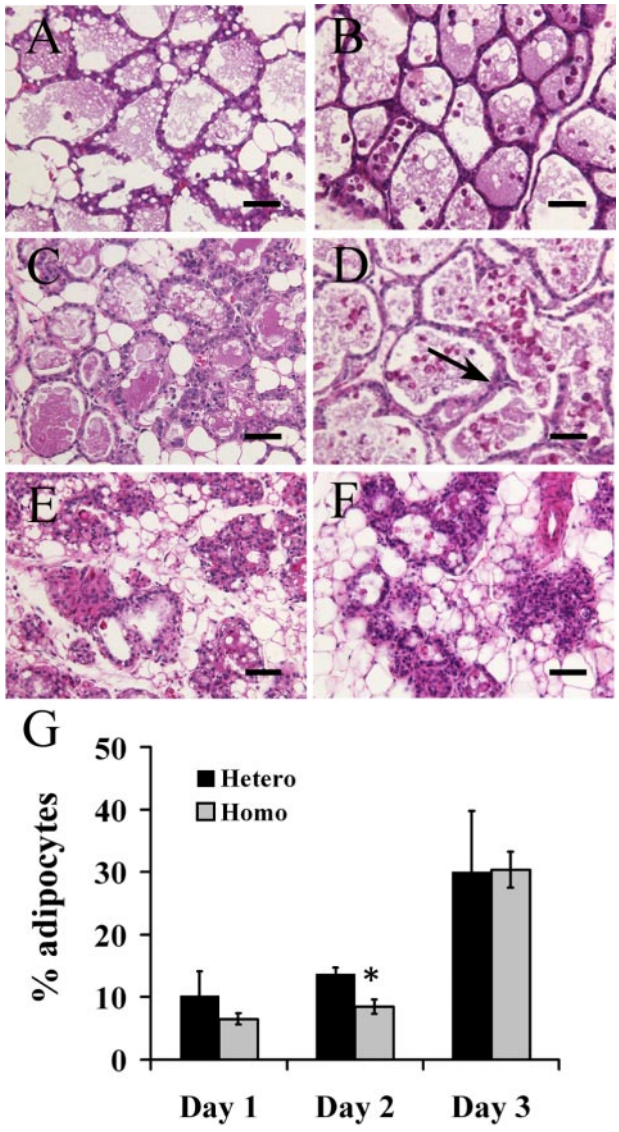

Figure 4. *Mfge8* mutant mice have a delay in alveolar collapse and adipocyte repopulation during early involution. (A–F) H & E sections of heterozygote controls (A, C, and E) and homozygous mutants (B, D, and F) from day 1 (A and B), day 2 (C and D), and day 3 (E and F) of involution. On day 2, the alveoli remain distended in homozygous mutants (arrow in D), and there are few adipocytes in the gland, compared with heterozygous controls (C). By day 3 of involution, the degree of alveolar collapse and proportion of adipocytes were similar in homozygous mutants (F) and heterozygous controls (E). (G) The proportion of fat in the mammary parenchyma on days 1 through 3 of involution was quantified by superimposing a grid on 10 randomly selected high power fields (100×) and counting intersections that marked adipocytes and epithelium. Heterozygote females had an increase in the percentage of adipocytes in the mammary glands parenchyma on day 2 of involution (n = 5 for each group, *$p < 0.01$. Data expressed as mean ± SEM). Bar, 0.2 mm.

nuclei on days 1 and 2 of involution. As epithelial cells undergo apoptosis they lose contact with the basement membrane and are shed into the alveolar lumens and subsequently ingested by phagocytes. To determine whether the increase in the number of apoptotic cells seen during the first 48 h of involution in *Mfge8* mutants was due to impaired apoptotic cell clearance rather than an increase in the number of cells undergoing apoptosis, we counted the number of apoptotic cells in the alveolar lumens versus the number of apoptotic cells in the alveolar epithelium. *Mfge8* mutants had significantly greater numbers of apoptotic cells within the alveolar lumens on both days 1 and 2 of involution (Figure 5D), but no difference in the number of apoptotic cells in the alveolar epithelium. To evaluate whether the

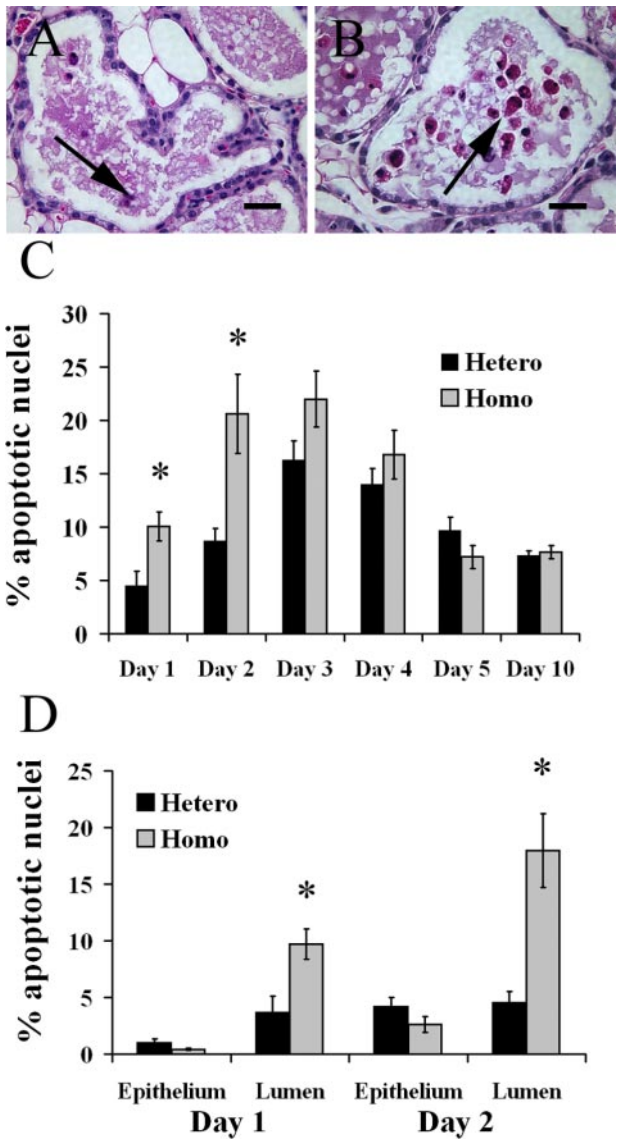

Figure 5. Increase in the number of apoptotic cells in the mammary gland epithelium of *Mfge8* mutant mice in early involution. (A and B) The percentage of apoptotic nuclei in homozygous mutants (B) and heterozygous controls (A) was quantified by counting the number of TUNEL positive cells on tissue sections and apoptotic bodies on H & E sections (arrows in A and B) from 14 randomly selected high power fields (400×). (C) Bar graph showing the percentage of apoptotic nuclei on days 1–5 and day 10 of involution ($n = 4–6$, * $p < 0.03$, data are expressed as mean ± SEM). (D) Bar graphs showing the percentage of apoptotic nuclei in the alveolar epithelium and alveolar lumen on days 1 and 2 of involution. *Mfge8* mutants had a significant increase in the number of apoptotic nuclei only in the alveolar lumens (arrows in A and B, $n = 4–6$, *$p < 0.03$ for day 1 and $p < 0.01$ for day 2 of involution). Bar, 0.1 mm.

increase in the apoptotic cells in the alveolar lumens represented a failure of viable epithelial cells to engulf these cells, we quantified the number of ingested apoptotic cells within alveolar epithelial cells on H & E sections from day 2 of involution. Alveolar epithelial cells from Mfge8 mutants had ingested significantly fewer apoptotic particles as compared with heterozygous controls (Figure 6, A and B). Analysis of sections stained with TUNEL assay provided similar results (unpublished data).

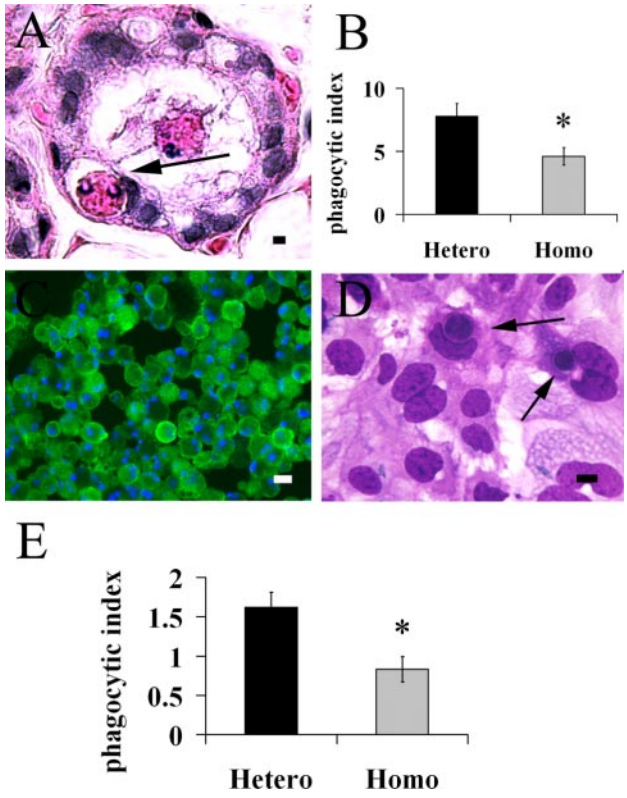

Figure 6. *Mfge8* mutants have impaired mammary gland epithelial cell phagocytosis in vivo and in vitro. (A and B) The number of ingested apoptotic particles (arrows in A) within alveolar epithelial cells was quantified (B) from 10 randomly selected fields (1000×) from day 2 of involution and expressed as the number of ingested particles multiplied by the percentage of epithelial cells counted (the phagocytic index). *Mfge8* mutants had a significantly lower phagocytic index ($n = 5$, *$p < 0.05$, data are expressed as mean ± SEM). (C) Apoptotic cells were obtained from the milk of involuting *Mfge8* mutant and control mice and stained with anti-activated caspase 3 antibody (green) and counterstained with DAPI (blue). (D) Apoptotic cells were incubated with PMEC for 5 h and the number of ingested cells (arrows in D) from 30 randomly selected fields (1000×) was quantified. (E) PMEC from heterozygous control mice incubated with heterozygous apoptotic cells had a significantly higher phagocytic index then PMEC from homozygous mice incubated with homozygous apoptotic cells ($n = 3$, *$p < 0.04$, data are expressed as mean ± SEM) Bar, 0.01 mm.

Epithelial Cells from Mfge8 *Mutant Mice Have Impaired Apoptotic Cell Clearance In Vitro*

To further evaluate the role of Mfge8 in epithelial cell-mediated apoptotic cell clearance, we evaluated the ability of primary mammary gland epithelial cells (PMEC) from *Mfge8* mutants and control mice to ingest apoptotic cells in vitro. We used apoptotic cells isolated from the milk of involuting *Mfge8* mutant and control mice as targets for phagocytosis in this assay. Apoptotic cells obtained by this method (milked apoptotic cells) were ~90% Annexin V-positive by FACS analysis (unpublished data) and virtually 100% apoptotic when stained with an anti-activated caspase 3 antibody (Figure 6C). PMEC from *Mfge8* mutant mice incubated with milked apoptotic cells from *Mfge8* mutant mice had a significantly lower phagocytic index then heterozygous PMEC incubated with milked apoptotic cells from heterozygous controls (Figure 6, D and E).

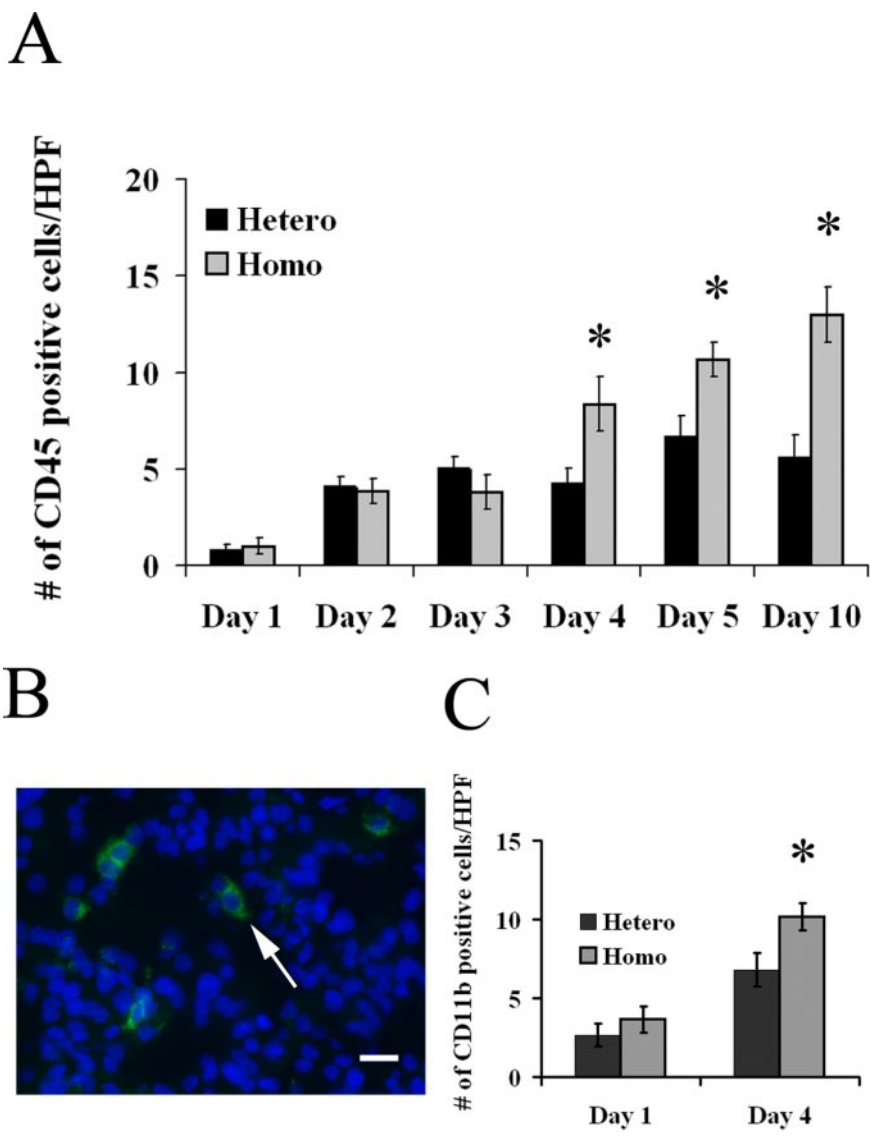

Figure 7. *Mfge8* mutants develop inflammation during involution. Immunohistochemical staining using anti-CD45 antibodies was done on selected days of involution in *Mfge8* mutants and heterozygote controls. (A) Bar graph showing the total numbers of CD45 positive cells per high-power field (400×) from 14 randomly selected fields. An increase in the number of inflammatory cells in *Mfge8* mutants was evident on day 4 of involution and persisted through day 10 ($n = 4–6$, $^*p < 0.03$ for day 4 and 5, and $^*p < 0.01$ for day 10). (B and C) Immunofluorescence staining using an anti-CD11b antibody (arrow in B) on mammary gland frozen sections from day 1 and day 4 of involution. (C) Bar graph showing an increase in CD11b-positive cells on day 4 of involution in homozygous females compared with heterozygous controls ($n = 4–5$, $^*p < 0.05$ for day 4, data are expressed as mean ± SEM). Bar, 0.1 mm.

Mfge8 *Mutants Develop Inflammation during Involution*

Given the increase in apoptotic cells, we hypothesized that *Mfge8* mutants may develop inflammation during involution. We therefore stained for CD45 antigen, a pan-leukocyte marker and counted the number of inflammatory cells in tissue sections. An increase in the number of CD45-positive cells was evident on day 4 and persisted on days 5 and 10 of involution (Figure 7A). To further characterize the inflammatory infiltrate, we stained frozen sections from day 1 and day 4 of involution with an anti-CD11b antibody (Figure 7, B and D), a marker found on activated phagocytes. As with the CD45 staining, we saw an increase in the number of cells expressing CD11b on day 4 of involution in homozygous mice.

Mfge8 *Mutant Mice Develop Progressive Mammary Gland Ductal Dilatation*

We next evaluated the long-term consequences of the alterations in mammary gland involution on mammary gland morphology. Homozygous females developed progressive ductal dilatation with successive pregnancies compared with heterozygote controls (Figure 8, A–D). Ductal dilatation was evident after one pregnancy but became much more dramatic after multiple pregnancies and was apparent in the primary ducts as well as the secondary and tertiary branches (Figure 8, F–H). Ductal dilatation did not occur due to aging because 9-mo-old virgin *Mfge8* mutant mice had normal ductal caliber (Figure 8, A and H). To assess whether heterozygous females had an intermediate phenotype compared with wild-type and homozygous females, we quantified ductal caliber in multiparous wild-type females (Figure 8H). Wild type females had similar ductal diameter after multiple pregnancies as compared with heterozygous females and significantly smaller ductal caliber as compared with homozygous females.

C/EBPβ and Epimorphin Expression Is Unchanged in Mfge8 *Mutant Mice*

We next evaluated expression of two genes shown to regulate ductal caliber. C/EBPβ is a nuclear transcription factor that plays a key role in mammary gland morphogenesis (Robinson *et al.*, 1998; Seagroves *et al.*, 1998) and *C/EBPβ* null mice have dilated mammary gland ducts (Seagroves *et al.*, 1998). Epimorphin is a stromal morphogenic factor that

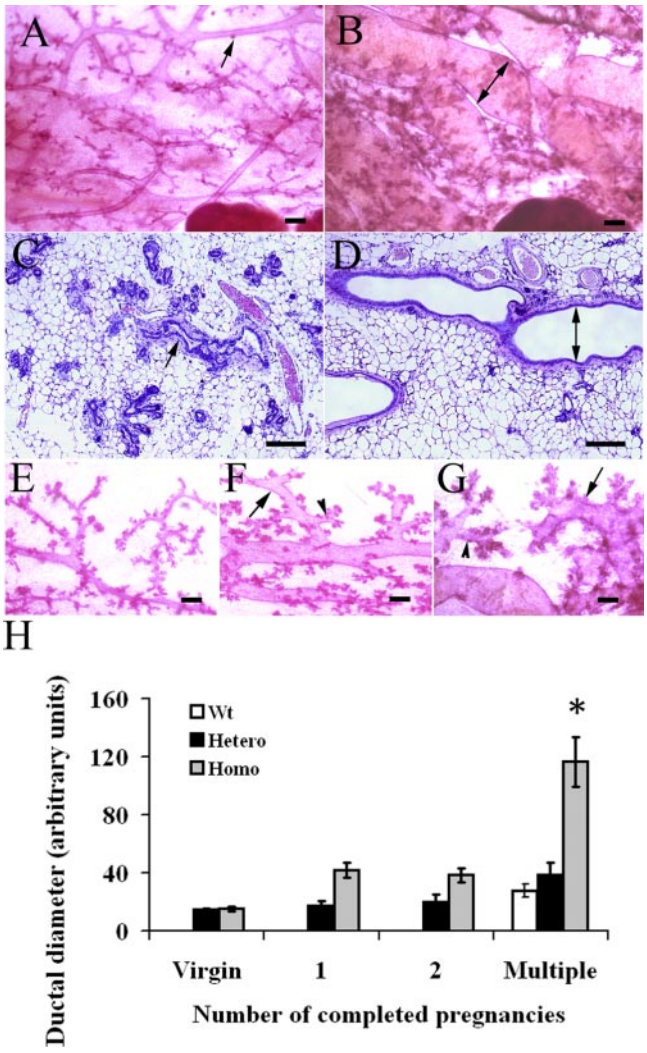

Figure 8. *Mfge8* mutant mice develop progressive ductal dilatation with successive pregnancies. (A and B) Whole mounts of mature virgin (A) and multiparous (B) homozygous female mice show massive dilatation of the ductal network in the multiparous female (double-headed arrow in B) but normal caliber ducts in the mature virgin (arrow in A). (C and D) H & E-stained tissue sections show normal caliber ducts in a multiparous heterozygote female (arrow in C) and massively dilated ducts in a multiparous homozygote female (double-headed arrow in D). (E–G) Whole mounts of mature virgin homozygote female (E), homozygote female after 1 pregnancy (F), and multiparous homozygote female (G). Ductal dilatation was most severe in the multiparous female (G) and in addition to the primary ducts seen in B also involved the secondary (arrows in F and G) and tertiary branches (arrowheads in F and G). (H) The degree of ductal dilatation was quantified by measuring the diameter of the largest primary duct adjacent to the central lymph node using NIH image software (NIH image 1.63). Ductal dilatation was present after 1 pregnancy and there was a threefold increase in ductal size after multiple (greater than 5) pregnancies ($n = 4$ for comparisons of 9-mo-old and virgin mice, $n = 3$ for comparisons of ductal size after 1 and 2 pregnancies, and $n = 5$ for comparisons of multiple pregnancies, *$p < 0.01$ when comparing multiparous homozygous females with multiparous heterozygous or wild-type females, data expressed as mean ± SEM) Bar, 0.2 mm.

causes ductal dilatation when expressed in the epithelium of transgenic mice under the whey acidic protein promoter (Hirai *et al.*, 2001). Epimorphin transgenic mice have altered expression of the C/EBPβ isoforms LAP and LIP. We hypothesized that Mfge8 could act upstream of these factors and that loss of Mfge8 might alter the expression or ratio of C/EBPβ isoforms or up-regulate epimorphin expression. However, C/EBPβ isoform expression and ratio and epimorphin protein levels were unchanged in *Mfge8* mutant mice during involution, pregnancy, and lactation (unpublished data).

DISCUSSION

In this report we show that Mfge8 plays a central role in mammary gland remodeling during involution. Mice homozygous for a gene trap insertion in *Mfge8* have normal mammary gland development during puberty, pregnancy, and lactation. During stage I of involution *Mfge8* mutants have impaired apoptotic cell clearance leading to inflammation and progressive distortion of the mammary gland ductal network. These studies identify a novel role for Mfge8 in mammary gland remodeling and demonstrate that Mfge8 targets apoptotic epithelial cells for phagocytosis.

Mammary gland involution is made up of an early stage (stage I, the first 48 h) and late stage (Wiseman and Werb, 2002). Stage I of involution is regulated by milk stasis within mammary gland parenchyma and is characterized by apoptosis of the secretory epithelium (Lund *et al.*, 1996; Li *et al.*, 1997; Furth, 1999; Wilde *et al.*, 1999). During the first 48 h of involution the basement membrane remains intact and lactation can resume if suckling is reinitiated (Li *et al.*, 1997; Furth, 1999; Wilde *et al.*, 1999). As epithelial cells undergo apoptotic cell death during involution, they are shed into the alveolar lumen where they are rapidly removed by phagocytosis. During involution Mfge8 is present on the milk membrane inside the alveolar and ductal lumens and on the apical surface of the epithelium (unpublished data). Both locations place Mfge8 in close apposition to apoptotic epithelial cells. *Mfge8* mutants had increased numbers of apoptotic cells in the alveolar lumens on day 1 and day 2 of involution, but no increase in the number of apoptotic cells in the remaining viable alveolar epithelium. These data suggest that the number of cells undergoing apoptosis in the mammary gland epithelium is unchanged in *Mfge8* mutants. However, the number of cells that have undergone apoptosis have been shed into the alveolar lumens and are available for engulfment is increased in *Mfge8* mutants, implicating an impairment in the ability of phagocytes to clear these cells. Impaired phagocytosis in *Mfge8* mutants is further supported by the decrease in the phagocytic index of the viable epithelial cells in vivo at the time when there is the greatest difference in the number of apoptotic cells within the alveolar lumens. In addition, primary mammary gland epithelial cells from *Mfge8* mutant mice have impaired phagocytosis in vitro. Therefore, it appears that mammary gland Mfge8 binds apoptotic epithelial cells shed into the alveolar lumen and targets these cells for engulfment. Without functional Mfge8, phagocytosis of apoptotic epithelial cells is impaired.

As involution progresses past 48 h, proteases are released that cleave the basement membrane and irreversible remodeling of the mammary gland takes place (Lund *et al.*, 1996). On day 3 and day 4 of involution there is continued programmed cell death of the remaining secretory epithelium (Strange *et al.*, 2001). The proportion of apoptotic cells in our *Mfge8* mutants was not significantly different from controls on day 3 or day 4 of involution despite the fact that the total proportion of apoptotic nuclei was greatest at this time. One possible explanation is that the failure to rapidly clear apoptotic cells in the first 48 h of involution triggers compensa-

tory pathways that augment clearance on days 3 and 4. Another possibility is that though the greatest proportion of apoptotic nuclei was seen on day 3 of involution, the size and epithelial content of the mammary gland is significantly less at this time than on day 1 or day 2 (unpublished data). Therefore, the absolute number of mammary gland epithelial cells undergoing apoptosis is greatest between 24 and 48 h after the onset of involution, the time at which Mfge8 mutants had the greatest excess of apoptotic cells.

The cells primarily responsible for clearance of apoptotic cells within the mammary gland are largely unknown. Some researchers favor nonprofessional phagocytes such as epithelial cells in stage 1 of involution and professional phagocytes such as macrophages in the second stage (Fadok, 1999; Stein *et al.*, 2004), whereas others discount a substantial role for inflammatory cells (Monks *et al.*, 2002, 2005). *Mfge8* mutants had a threefold excess of apoptotic nuclei on day 2 of involution, but clearance had apparently caught up with that in heterozygotes by day 3. It would be tempting to speculate that the increase in inflammatory cells that we observed in involuting *Mfge8* mutant mammary glands was responsible for this effect, but this increase was not apparent until day 4 of involution. The paucity of immune cells in the mammary glands at the time of impaired apoptotic cell clearance in combination with the impaired phagocytic capacity of mammary gland epithelial cells suggest that epithelial cells utilize Mfge8 for apoptotic cell clearance. Therefore, our data suggest that epithelial cells utilizing Mfge8 mediate a significant proportion of apoptotic cell clearance during the first 48 h of involution. As the number of immune cells infiltrating the mammary gland increases with involution, the relative contribution of professional phagocytes to apoptotic cell clearance likely predominates.

The orderly removal of apoptotic cells is necessary to avoid the inflammatory response that accompanies the release of antigens by dying cells (Savill and Fadok, 2000; Hengartner, 2001; Geske *et al.*, 2002). Our line of *Mfge8* mutants developed inflammation during involution that persisted at least until day 10. After involution, *Mfge8* mutants developed distortion of the mammary gland architecture and with multiple cycles of pregnancy, involution, and inflammation developed dramatic dilatation of the mammary gland ductal network. On the basis of the data in the present study we cannot determine whether these progressive abnormalities in ductal architecture were a consequence of delayed clearance of apoptotic cells, increased numbers of inflammatory cells or both.

Mammary gland ductal dilatation is a rare phenotype seen in a few other genetically altered mice (Hirai *et al.*, 1998; Seagroves *et al.*, 1998; Vogel *et al.*, 2001). Transgenic mice that express epimorphin in the mammary gland epithelium under the whey acidic protein promoter have ductal dilatation and an abnormal ratio of the C/EBPβ isoforms (Hirai *et al.*, 2001). *C/EBPβ* null mice also have pubertal ductal dilatation (Seagroves *et al.*, 1998). However we found no differences in LAP/LIP and epimorphin expression during pregnancy, lactation, and involution in *Mfge8* mutants or controls. Thus, the ductal dilatation seen in *Mfge8* mutant mice appeared not to be mediated by the C/EBPβ isoforms LAP or LIP or epimorphin.

Our line of *Mfge8* mutants were generated using a gene trapping vector that disrupts *Mfge8* and produces a fusion protein that is retained in the endoplasmic reticulum and is rapidly degraded (Mitchell *et al.*, 2001; Silvestre *et al.*, 2005). Though we cannot exclude the possibility that the fusion protein may have had deleterious effects on the mammary gland, our comparison of multiparous wild-type and heterozygous females revealed minimal differences in ductal morphology. This suggests that the fusion protein was not responsible for the phenotype we observed in the mammary glands of homozygous females. In addition, our mutants had phenotypes similar to traditional *Mfge8* knockouts described in the literature (Ensslin and Shur, 2003; Hanayama *et al.*, 2004; Silvestre *et al.*, 2005), and our fusion protein was trapped intracellularly and not secreted into the alveolar or ductal lumens, the locations where we found impaired apoptotic cell clearance and architectural distortion with progressive pregnancies.

ACKNOWLEDGMENTS

We thank Peter Henson for helpful discussions regarding this project, Kevin Mitchell for providing the HST227 ES cells, and Matthew Binnie, Mark Travis, and Greg deHart for technical expertise. This work was supported in part by National Institutes of Health fellowship 1F32HL073530–01 (K.A.), Program in Genomics Applications Grant U01 HL66600 (BayGenomics), Grants HL64353, HL56385, and HL53949 from the National Heart, Lung, and Blood Institute (D.S.), CA57621 and ES12801 from the National Institute of Environmental Health Sciences and the National Cancer Institute (Z.W.), and the National Science Foundation student training Grant CSU LS-AMP HRD-0350008 (R.F.).

REFERENCES

Carmon, L. *et al.* (2002). Characterization of novel breast carcinoma-associated BA46-derived peptides in HLA-A2.1/D(b)-beta2m transgenic mice. J. Clin. Invest. *110*, 453–462.

Ensslin, M. A., and Shur, B. D. (2003). Identification of mouse sperm SED1, a bimotif EGF repeat and discoidin-domain protein involved in sperm-egg binding. Cell *114*, 405–417.

Fadok, V. A. (1999). Clearance: the last and often forgotten stage of apoptosis. J. Mammary Gland Biol. Neoplasia *4*, 203–211.

Furth, P. A. (1999). Introduction: mammary gland involution and apoptosis of mammary epithelial cells. J. Mammary Gland Biol. Neoplasia *4*, 123–127.

Geske, F. J., Monks, J., Lehman, L., and Fadok, V. A. (2002). The role of the macrophage in apoptosis: hunter, gatherer, and regulator. Int. J. Hematol. *76*, 16–26.

Hanayama, R., Tanaka, M., Miwa, K., Shinohara, A., Iwamatsu, A., and Nagata, S. (2002). Identification of a factor that links apoptotic cells to phagocytes. Nature *417*, 182–187.

Hanayama, R., Tanaka, M., Miyasaka, K., Aozasa, K., Koike, M., Uchiyama, Y., and Nagata, S. (2004). Autoimmune disease and impaired uptake of apoptotic cells in MFG-E8-deficient mice. Science *304*, 1147–1150.

Hengartner, M. O. (2001). Apoptosis: corralling the corpses. Cell *104*, 325–328.

Hirai, Y., Lochter, A., Galosy, S., Koshida, S., Niwa, S., and Bissell, M. J. (1998). Epimorphin functions as a key morphoregulator for mammary epithelial cells. J. Cell Biol. *140*, 159–169.

Hirai, Y., Radisky, D., Boudreau, R., Simian, M., Stevens, M. E., Oka, Y., Takebe, K., Niwa, S., and Bissell, M. J. (2001). Epimorphin mediates mammary luminal morphogenesis through control of C/EBPbeta. J. Cell Biol. *153*, 785–794.

Humphreys, R. C. (1999). Programmed cell death in the terminal endbud. J. Mammary Gland Biol. Neoplasia *4*, 213–220.

Humphreys, R. C., Krajewska, M., Krnacik, S., Jaeger, R., Weiher, H., Krajewski, S., Reed, J. C., and Rosen, J. M. (1996). Apoptosis in the terminal endbud of the murine mammary gland: a mechanism of ductal morphogenesis. Development *122*, 4013–4022.

Ikeda, K., Kato, M., Yamanouchi, K., Naito, K., and Tojo, H. (2002). Novel development of mammary glands in the nursing transgenic mouse ubiquitously expressing WAP gene. Exp. Anim. *51*, 395–399.

Larocca, D., Peterson, J. A., Urrea, R., Kuniyoshi, J., Bistrain, A. M., and Ceriani, R. L. (1991). A Mr 46,000 human milk fat globule protein that is highly expressed in human breast tumors contains factor VIII-like domains. Cancer Res. *51*, 4994–4998.

Li, M., Liu, X., Robinson, G., Bar-Peled, U., Wagner, K.U., Young, W.S., Hennighausen, L., and Furth, P.A. (1997). Mammary-derived signals activate programmed cell death during the first stage of mammary gland involution. Proc. Natl. Acad. Sci. USA *94*, 3425–3430.

Lonnerdal, B. (2003). Nutritional and physiologic significance of human milk proteins. Am. J. Clin. Nutr. *77*, 1537S–1543S.

Lund, L. R., Romer, J., Thomasset, N., Solberg, H., Pyke, C., Bissell, M. J., Dano, K., and Werb, Z. (1996). Two distinct phases of apoptosis in mammary gland involution: proteinase-independent and -dependent pathways. Development *122*, 181–193.

Mather, I. H. (1987). The mammary Gland, Development, Regulation, and Function, New York: Plenum Publishing.

Mitchell, K. J. *et al.* (2001). Functional analysis of secreted and transmembrane proteins critical to mouse development. Nat. Genet. *28*, 241–249.

Monks, J., Geske, F. J., Lehman, L., and Fadok, V. A. (2002). Do inflammatory cells participate in mammary gland involution? J. Mammary Gland Biol. Neoplasia *7*, 163–176.

Monks, J., Rosner, D., Geske, F. J., Lehman, L., Hanson, L., Neville, M. C., and Fadok, V. A. (2005). Epithelial cells as phagocytes: apoptotic epithelial cells are engulfed by mammary alveolar epithelial cells and repress inflammatory mediator release. Cell Death Differ. *12*, 107–114.

Oshima, K., Aoki, N., Negi, M., Kishi, M., Kitajima, K., and Matsuda, T. (1999). Lactation-dependent expression of an mRNA splice variant with an exon for a multiply O-glycosylated domain of mouse milk fat globule glycoprotein MFG-E8. Biochem. Biophys. Res. Commun. *254*, 522–528.

Robinson, G. W., Johnson, P. F., Hennighausen, L., and Sterneck, E. (1998). The C/EBPbeta transcription factor regulates epithelial cell proliferation and differentiation in the mammary gland. Genes Dev. *12*, 1907–1916.

Savill, J., and Fadok, V. (2000). Corpse clearance defines the meaning of cell death. Nature *407*, 784–788.

Seagroves, T. N., Krnacik, S., Raught, B., Gay, J., Burgess-Beusse, B., Darlington, G. J., and Rosen, J. M. (1998). C/EBPbeta, but not C/EBPalpha, is essential for ductal morphogenesis, lobuloalveolar proliferation, and functional differentiation in the mouse mammary gland. Genes Dev. *12*, 1917–1928.

Shamay, A., Pursel, V. G., Wilkinson, E., Wall, R. J., and Hennighausen, L. (1992). Expression of the whey acidic protein in transgenic pigs impairs mammary development. Transgenic Res. *1*, 124–132.

Silvestre, J. S. *et al.* (2005). Lactadherin promotes VEGF-dependent neovascularization. Nat. Med. *11*, 499–506.

Stein, T., Morris, J. S., Davies, C. R., Weber-Hall, S. J., Duffy, M. A., Heath, V. J., Bell, A. K., Ferrier, R. K., Sandilands, G. P., and Gusterson, B. A. (2004). Involution of the mouse mammary gland is associated with an immune cascade and an acute-phase response, involving LBP, CD14 and STAT3. Breast Cancer Res. *6*, R75–R91.

Strange, R., Metcalfe, T., Thackray, L., and Dang, M. (2001). Apoptosis in normal and neoplastic mammary gland development. Microsc. Res. Tech. *52*, 171–181.

Stubbs, J. D., Lekutis, C., Singer, K. L., Bui, A., Yuzuki, D., Srinivasan, U., and Parry, G. (1990). cDNA cloning of a mouse mammary epithelial cell surface protein reveals the existence of epidermal growth factor-like domains linked to factor VIII-like sequences. Proc. Natl. Acad. Sci. USA *87*, 8417–8421.

Vogel, W. F., Aszodi, A., Alves, F., and Pawson, T. (2001). Discoidin domain receptor 1 tyrosine kinase has an essential role in mammary gland development. Mol. Cell Biol. *21*, 2906–2917.

Wilde, C. J., Knight, C. H., and Flint, D. J. (1999). Control of milk secretion and apoptosis during mammary involution. J. Mammary Gland Biol. Neoplasia *4*, 129–136.

Wiseman, B. S., and Werb, Z. (2002). Stromal effects on mammary gland development and breast cancer. Science *296*, 1046–1049.